

# Localized Parameter Shifts from GONG+ data

R. Howe<sup>1</sup>, J. Bolding<sup>1</sup>, T. Corbard<sup>2</sup>, F. Hill<sup>1</sup>, R. Komm<sup>1</sup>, C. Toner<sup>1</sup>

<sup>1</sup> National Solar Observatory, Tucson AZ

<sup>2</sup> Observatoire de la Côte d'Azur, Nice, France

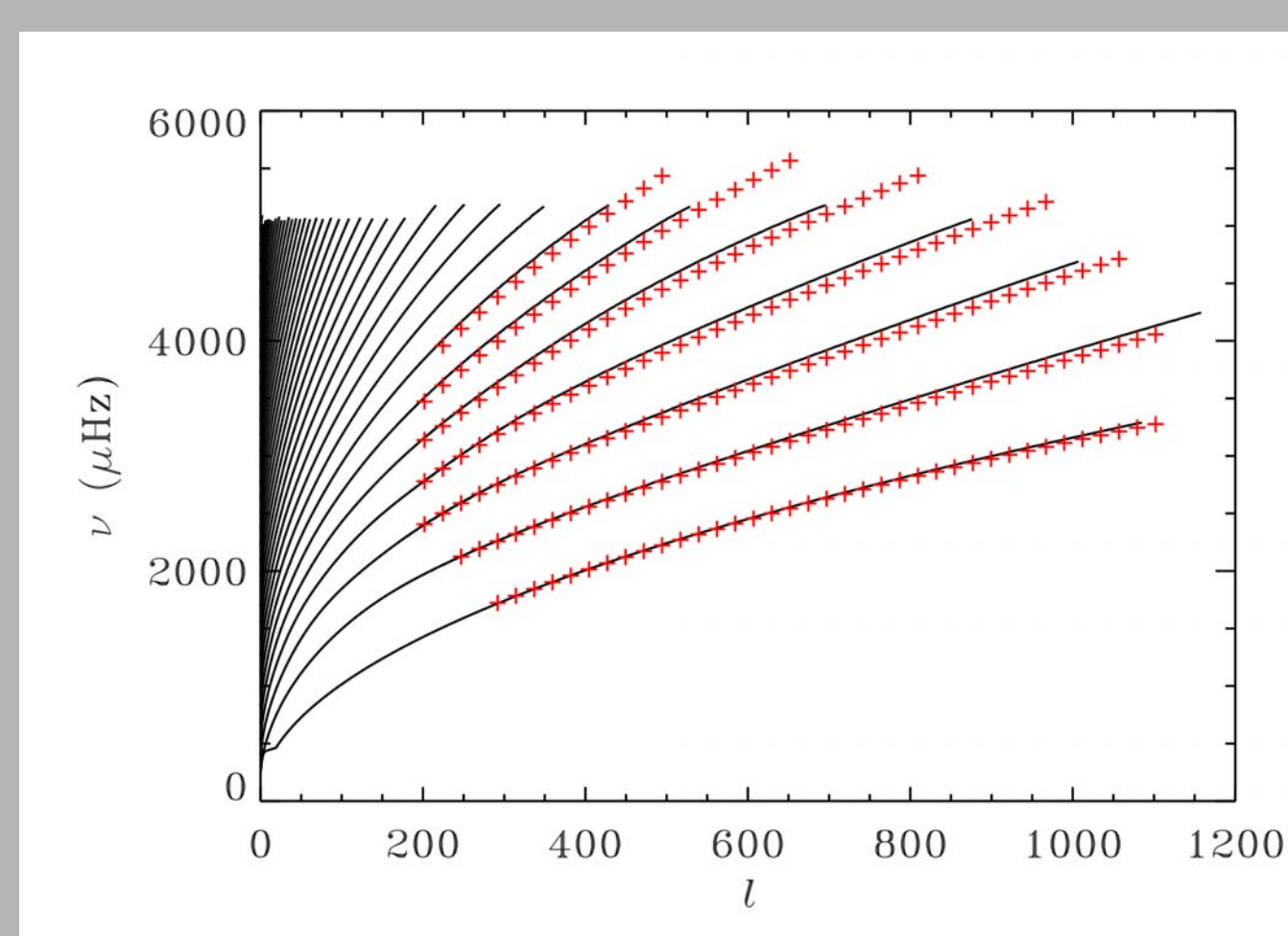
## INTRODUCTION

The ring diagram technique of local helioseismology uses 3-dimensional power spectra from small patches of the solar disk to follow local flows below the surface and monitor local near-surface changes in high-degree modes. Such analysis (Hill, 1988) has previously been extensively used on the 'Dynamics' (full-field, 1024x1024-pixel) data from the MDI instrument aboard SOHO (see, for example, Haber et al. 2002). Upgraded cameras now allow similar data to be taken year-round from the six stations of the GONG network. Systematic analysis of this data has now begun.

In this poster, we show the results of preliminary analysis of the mode frequencies, widths and heights obtained from GONG for Carrington Rotation 1988 (April 2002). All three quantities show a clear variation with the surface magnetic flux, consistent with results from global p-modes.

## THE DATA

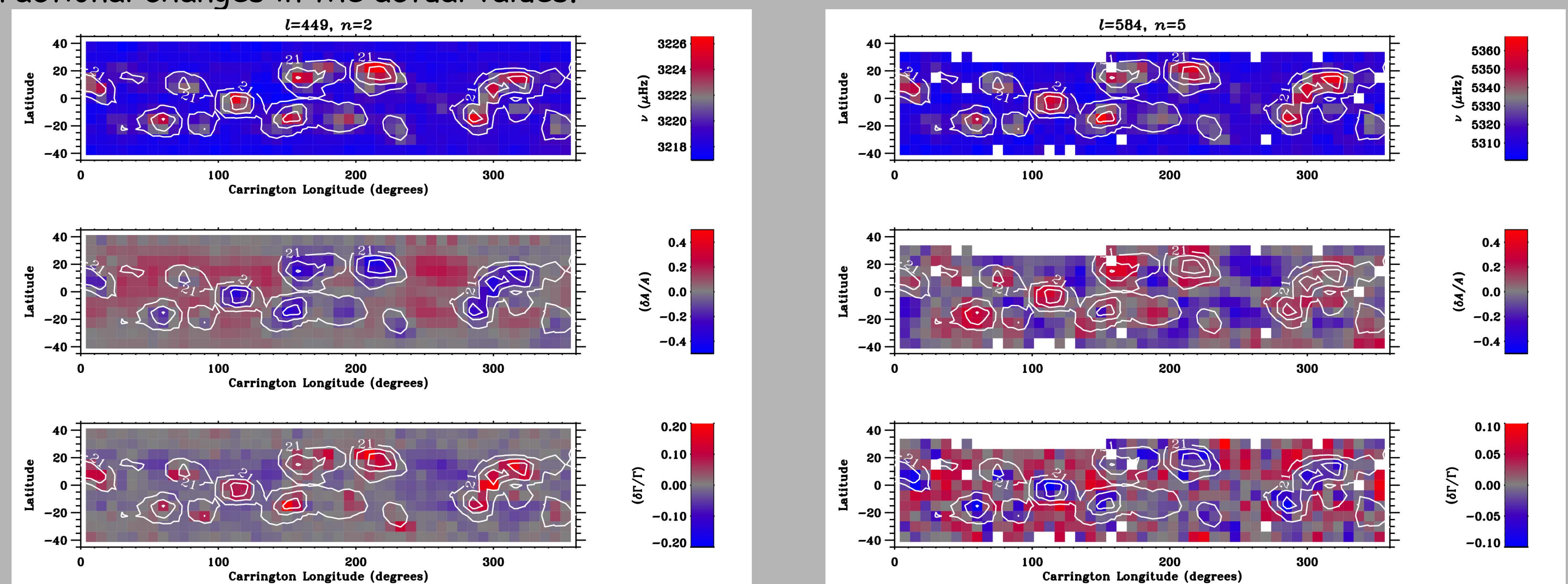
For each 1664-minute 'day', we analyze 189 15°-square patches, with centers spaced by 7.5°, as in the dense-pack analysis of Haber et al. The modes, of radial order  $0 \leq n \leq 6$ , are fitted as Lorentzian peaks of height  $A$ , width  $\Gamma$  and frequency  $\nu$ , at spatial wavelengths separated by approximately 22.5 in degree  $l$ . Only modes which are successfully fitted in at least 30% of the available 4912 patches are used in this analysis. This yields modes with  $l$  between 200 and 970 and frequencies between 1700 and 5400  $\mu\text{Hz}$ .



The  $l$ - $\nu$  diagram above shows the modes overlaid on model frequencies from Model S of Christensen-Dalsgaard (1996). The deepest-penetrating modes have lower turning points at about  $0.95R$ . Notice that some modes ('pseudomodes') lie above the theoretical acoustic cutoff, where this model makes no predictions.

## RESULTS

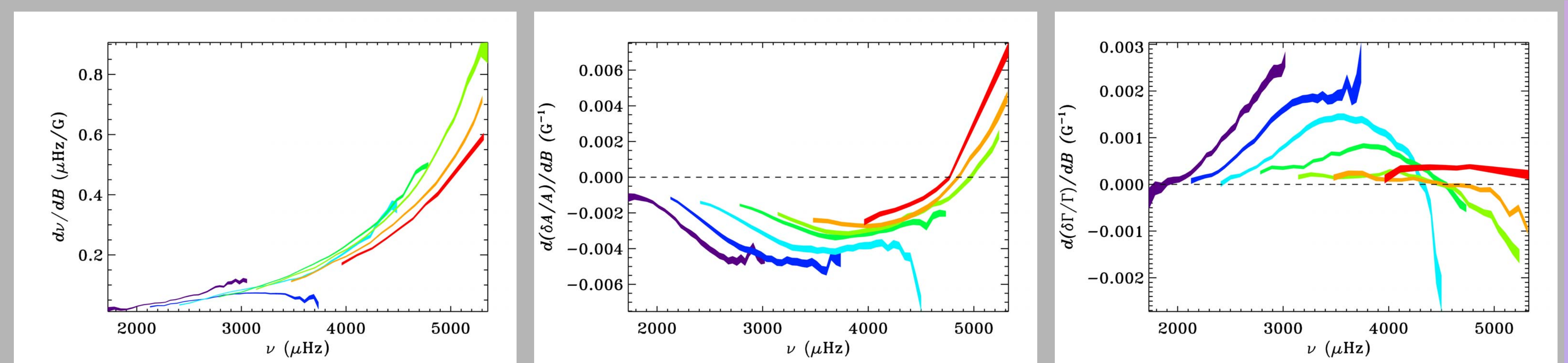
In order to study the parameter shifts, a 2-dimensional quadratic function of the longitudinal and latitudinal distances from disk center was fit over the whole rotation for each mode and subtracted from the raw values. In the case of the amplitude and width, the mean value for each day was also subtracted to allow for variations in duty cycle, etc. The results were then formed into synoptic maps and compared with the gross magnetic flux from the Kitt Peak synoptic data, averaged over the same 15° squares. For  $A$  and  $\Gamma$ , we consider changes in the natural logarithm of the quantities, corresponding to fractional changes in the actual values.



Over much of the range covered, the parameters show a linear relationship to the local magnetic index; in active regions, the mode frequency and width increase and the mode height decreases, as shown in the example synoptic maps above left for  $l=449$ ,  $n=2$ . Similar trends have been seen in the global modes (e.g., Komm, Howe, & Hill 2002, Howe, Komm, & Hill 2002).

For some of the highest-frequency modes, the trends for height and width reverse, as shown in the example at right ( $l=584$ ,  $n=5$ ). The blank squares are those where the fit failed for this mode. These modes are believed to lie above the acoustic cutoff frequency and not be trapped at the surface.

The sensitivity plots below show the slopes of linear regressions between magnetic index and frequency (left), fractional mode height change (middle) and fractional width change (right). The ridges are color-coded from  $n=0$  (indigo) to  $n=6$  (red).



There are some intermediate cases where the variation of height and width with magnetic index is not monotonic, with height being enhanced at low indices and suppressed at higher ones, and vice versa for line width. We speculate that this is a result of such modes becoming trapped again at higher magnetic indices, as the critical frequency (presumably related to the acoustic cutoff) increases.

Similar trends have been seen by Hindman et al. (2000) for frequency, Hindman and Brown (1998) for mode power, and by Rajaguru et al. (2001) for all parameters.

A more thorough study of the parameter variations, using MDI data from 1996-2002, is in preparation (Howe, Haber, Hindman et al, 2004)

## References

- Christensen-Dalsgaard, J., et al. 1996, *Science*, 272, 1286
- Haber, D. A., Hindman, B. W., Toomre, J., Bogart, R. S., Larsen, R. M., & Hill, F. 2002, *ApJ*, 570, 885
- Hill, F. 1988, *ApJ*, 339, 996
- Hindman, B., Haber, D. A., Toomre, J., & Bogart, R. 2000, *SolPhys*, 193, 363
- Hindman, B., & Brown, T., 1998, *ApJ*, 504, 1029
- Howe, R., Komm, R. W., & Hill, F. 2002, *ApJ*, 580, 1172
- Komm, R., Howe, R., & Hill, F. 2002, *ApJ*, 572, 663
- Rajaguru, P., Basu, S., & Antia, H.M. 2001, *ApJ*, 563, 410



## Acknowledgments

This work utilizes data obtained by the Global Oscillation Network Group (GONG) project, managed by the National Solar Observatory, which is operated by AURA, Inc. under a cooperative agreement with the National Science Foundation. The data were acquired by instruments operated by the Big Bear Solar Observatory, High Altitude Observatory, Learmonth Solar Observatory, Udaipur Solar Observatory, Instituto de Astrofísica de Canarias, and Cerro Tololo Interamerican Observatory. RH is supported in part by NASA contract S-92698-F, which also supported RWK. The ring-diagram analysis package was partly developed by D. Haber, B. Hindman and R. M. Larsen, supported by NASA and Stanford University. NSO/Kitt Peak magnetic data used here are produced cooperatively by NSF/NOAO, NASA/GSFC and NOAA/SEL.